Journal of Rock Mechanics and Geotechnical Engineering 16 (2024) 1373–1387

Contents lists available at ScienceDirect

Journal of Rock Mechanics and Geotechnical Engineering

journal homepage: www.jrmge.cn

Full Length Article

A modified back analysis method for deep excavation with multi-objective optimization procedure

Chenyang Zhao [a,b], Le Chen [b], Pengpeng Ni [b,c], Wenjun Xia [d], Bin Wang [a,*]

[a] State Key Laboratory of Geomechanics and Geotechnical Engineering, Institute of Rock and Soil Mechanics, Chinese Academy of Sciences, Wuhan, 430071, China
[b] Guangdong Research Center for Underground Space Exploitation Technology, School of Civil Engineering, Sun Yat-sen University, Guangzhou, 510275, China
[c] Southern Marine Science and Engineering Guangdong Laboratory (Zhuhai), Zhuhai, 519000, China
[d] Jiangsu Provincial Transportation Engineering Construction Bureau, Nanjing, 210004, China

ARTICLE INFO

Article history:
Received 1 February 2023
Received in revised form
25 April 2023
Accepted 15 May 2023
Available online 3 July 2023

Keywords:
Multi-objective optimization
Back analysis
Surrogate model
Multi-objective particle swarm optimization (MOPSO)
Deep excavation

ABSTRACT

Real-time prediction of excavation-induced displacement of retaining pile during the deep excavation process is crucial for construction safety. This paper proposes a modified back analysis method with multi-objective optimization procedure, which enables a real-time prediction of horizontal displacement of retaining pile during construction. As opposed to the traditional stage-by-stage back analysis, time series monitoring data till the current excavation stage are utilized to form a multi-objective function. Then, the multi-objective particle swarm optimization (MOPSO) algorithm is applied for parameter identification. The optimized model parameters are immediately adopted to predict the excavation-induced pile deformation in the continuous construction stages. To achieve efficient parameter optimization and real-time prediction of system behavior, the back propagation neural network (BPNN) is established to substitute the finite element model, which is further implemented together with MOPSO for automatic operation. The proposed approach is applied in the Taihu tunnel excavation project, where the effectiveness of the method is demonstrated via the comparisons with the site monitoring data. The method is reliable with a prediction accuracy of more than 90%. Moreover, different optimization algorithms, including non-dominated sorting genetic algorithm (NSGA-II), Pareto Envelope-based Selection Algorithm II (PESA-II) and MOPSO, are compared, and their influences on the prediction accuracy at different excavation stages are studied. The results show that MOPSO has the best performance for high dimensional optimization task.

1. Introduction

In the process of deep excavation, controling the displacement of retaining pile within a predefined tolerance limit is crucial for construction safety (Wang et al., 2022). Reliable prediction of excavation-induced ground movement and pile deflection is one of the effective solutions (Kung et al., 2009). However, due to the uncertainties embedded in the soil profiles, it is generally difficult to determine the soil properties accurately. To address this problem, many researchers have developed the back analysis approach for soil parameter identification and subsequent construction parameter optimization.

Optimization algorithm can determine the soil and construction parameters through back analysis using field measurements. Zhu et al. (1998) combined the two-dimensional (2D) finite element model (FEM) and inverse analysis algorithm to optimize the parameters, which can be used to predict the real-time surface settlements and deformation of supporting piles during deep excavation. Zhao et al. (2015) applied the differential evolution algorithm in the deep excavation project of Taipei State-owned Enterprise Center (TENC), and effectively identified the suitable soil parameters. Stone et al. (2023) applied the back analysis method in design of pile length of a new composite foundation system, so-called caliche stiffened pile. Application of genetic algorithm (GA) in back analysis can be found in previous studies (Zhu and Liu, 2003; Park et al., 2015).

When conducting back analysis together with finite element modeling, intensive evaluations with finite element simulations are required, which can significantly reduce the efficiency of

* Corresponding author.
E-mail address: bwang@whrsm.ac.cn (B. Wang).
Peer review under responsibility of Institute of Rock and Soil Mechanics, Chinese Academy of Sciences.

https://doi.org/10.1016/j.jrmge.2023.05.007

optimization and prediction. Hence, it cannot guide the real-time deep excavation in practice. Many researchers proposed surrogate modeling to substitute the time-consuming numerical calculation, which can significantly improve the computational efficiency. Jiang et al. (2011) used support vector machine (SVM) to establish the correlation between geological parameters and soil displacement, which serves as a surrogate model in subsequent parameter back analyses. A deep learning algorithm, called embedded fully convolutional neural network (EF–CNN), was proposed by Gao et al. (2020) to replace the finite difference method for predicting the in situ stresses using a strain-softening model. Comparison with the experimental results indicated that their approach was stable and robust. He et al. (2021) combined the finite element method, neural network and random field theory to study the effect of soil uncertainty, the framework of which could cover the entire range of soil profiles, and its applicability was significantly improved. Zhang et al. (2021) used grey correlation analysis and set pair analysis (SPA) to determine the influencing factors of landslide problems. Zhao et al. (2023) applied three types of machine learning algorithms (random forest, SVM and artificial neural network) to correlate soil layer distribution and tunneling induced ground movement. Other models include least squares support vector machine (LSSVM) (Xue, 2017), back propagation neural network (BPNN) combined with particle swarm optimization (PSO) algorithm (Mohamad et al., 2018), surrogate modeling applied in back analysis with BPNN (Tao et al., 2019), grey correlation analysis (Tao et al., 2019), and Adaptive neuro-fuzzy inference system (ANFIS) (Liu et al., 2021).

Normally, there are different types of measurements in a real project of deep excavation, such as the horizontal and vertical displacements of retaining pile and the ground domain. When different types of measurements are adopted in back analysis, one has to address the multi-objective optimization task. A semi-empirical polynomial model has been developed by Zhang et al. (2015) for updating the soil parameters and predicting the maximum deflection of retaining walls. Through seven case studies, the model accuracy has been improved to be above 80%. Sun et al. (2018) combined BPNN and non-dominated sorting genetic algorithm (NSGA-II) algorithm to back-calculate the soil parameters based on the measured displacements in three directions, and they further used the identified soil parameters to predict the soil deformation. Their results show that the prediction accuracy can reach more than 90%. Jiang et al. (2018a) pointed out that the uncertainty of geological information has an adverse impact on slope stability, and they adopted the Bayesian updating method to reduce the uncertainty. Jiang et al. (2018b) combined BPNN with vector evaluated genetic algorithm (VEGA) to identify the geological and mechanical parameters for a deep excavation problem. A new algorithm called enhanced multi-objective differential evolution (EMODE) was proposed by Jin et al. (2019), where a two-objective optimization task was established by using lateral wall deflection and ground movement in a real project. Some scholars considered different constitutive models as variables in back analysis (Jin et al., 2020). Tao et al. (2022) used the Kriging method to establish a surrogate model of finite element, and adopted the MOPSO method for parameter optimization. Hong et al. (2023) provided an advanced reliability design method, in which the point estimating method (PEM) and multi-objective optimization algorithm were used to optimize the parameters, showing a higher efficiency than the NSGA-II algorithm.

As deep excavation is constructed in several stages, there are continuous recordings of different types of measurements. In previous studies, researchers normally selected a certain excavation stage to conduct parameter optimization (Sun et al., 2018). This is the so-called stage-by-stage model validation, which cannot guide the real construction, when reliable and efficient predictions are necessarily required.

This paper develops a modified back analysis method with multi-objective optimization procedure. The field measured horizontal displacements of retaining piles in each excavation stage (time series data) are utilized to form a multi-objective function, which makes full use of the available data and improves the accuracy of parameter optimization, since more data can be obtained with deeper excavation. It is worth mentioning that in practice, ensuring the stability of two or more types of monitoring data simultaneously is challenging, and as such a single type of monitoring data is adopted in the proposed approach. Therefore, the proposed approach is less sensitive to the monitoring data compared to previous multi-objective optimization procedures, where the use of several types of real measurements can involve different uncertain degrees. Furthermore, the BPNN surrogate model is implemented in the proposed approach to substitute numerical simulation, which significantly improves the efficiency of back analysis and parameter optimization. In this way, the real-time prediction of pile displacement during excavation is available and affordable.

2. Method

Fig. 1 shows the proposed multi-objective optimization framework, which contains four levels. Level 1 establishes the surrogate model using the Latin hypercube sampling (LHS) method together with finite element simulation. In Level 2, the surrogate model performance is evaluated based on the field measurements. The establishment and the resolution of multi-objective optimization task are conducted in Level 3. Finally, online prediction is achieved in Level 4. Detailed descriptions for each level are given in the following subsections.

2.1. Surrogate modeling

The procedures of establishing the surrogate model mainly include: (1) parameters sampling using the LHS method, (2) evaluation of the FEM using the sampling parameters, and (3) establishment of BPNN using sampling parameters as input and numerical results as output.

2.1.1. Parameters sampling

According to previous studies (Song et al., 2004; Jiang et al., 2007), the main factors affecting the deformation of retaining piles are stratum parameters (i.e. elastic modulus E, cohesion c, and internal friction angle φ) (Cao et al., 2017; Feng et al., 2022), structural parameters (i.e. supporting strut stiffness) (Qian et al., 2011; Zhao et al., 2015), and construction parameters (i.e. excavation depth in each stage) (Wu et al., 2021). Hence, these parameters are selected as the variables in the present study, and the LHS method is utilized to generate 200 sets of parameters combination.

2.1.2. Evaluation of finite element model (FEM)

The FEM of deep excavation is created based on the design documents and geotechnical report. The numerical results are compared with the field measurements for model evaluation. After that, the parameter samples generated in the previous step are applied in the calibrated model for iterative calculations, and the numerical results (i.e. displacement of retaining pile and axial force of support strut) are extracted.

2.1.3. Establishment of BPNN

The BPNN (Rumelhart et al., 1986) is the most widely-applied machine learning algorithm. It generally consists of three layers,

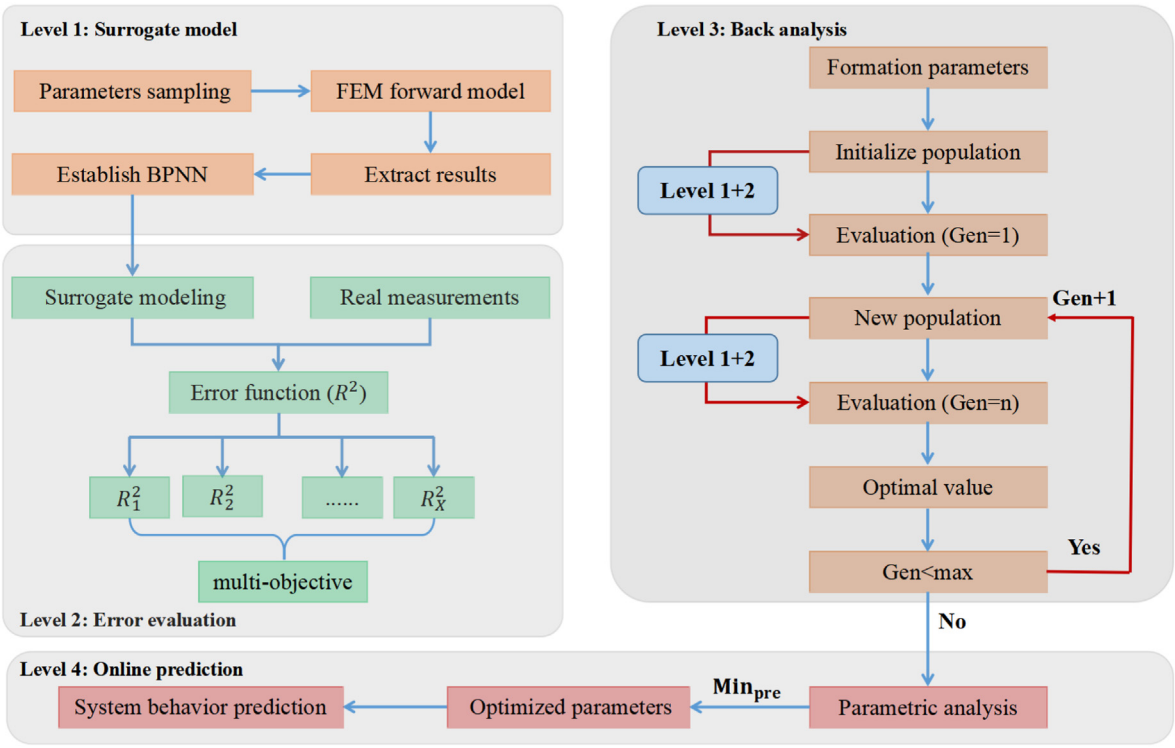

Fig. 1. Proposed multi-objective optimization framework.

i.e. input layer, hidden layer and output layer. The hidden layer transfers important information between the input layer and the output layer. BPNN is normally composed of multiple hidden layers, which can realize the modeling of complex problems.

In this paper, the input of neural network includes stratum parameters, structural parameters and excavation parameters. The horizontal displacements of retaining pile at each excavation stage are taken as the output. When the network training accuracy reaches more than 90%, the established BPNN model can, in general, replace the finite element model, thereby improving the computational efficiency of later model evaluation and prediction. The specific framework is shown in Fig. 10.

Fig. 2. Satellite view and site construction photo of Taihu tunnel.

2.2. Error evaluation

In previous studies, most error functions were defined as summation of squares due to regression (SSR), mean square error (MSE), or root mean square error (RMSE) (Qian et al., 2019). In this paper, in order to more intuitively evaluate the fitting effect of measurements and back analysis results, the term of R^2 is defined as follows:

$$R^2 = 1 - \frac{\sum (u_i - v_i)^2}{\sum (u_i - v_i)^2 + \sum (v_i - \overline{u})^2} \tag{1}$$

where u_i is the measurement at the i th observation point; $\overline{u}$ is the average value of the measurements at all monitoring points; and v_i is the predicted value using the surrogate model.

The closer the term R^2 approaches 1, the higher the fitting accuracy is. Within this framework, the evaluation error until j th excavation stage is defined as

$$Z_j = 1 - R_j^2 \tag{2}$$

where R_j is coefficient of determination at jth excavation stage.

When it comes to multiple excavation stages, it is necessary to formulate a total error function. The generalized objective function can be expressed as a multi-objective optimization form:

$$\min[\boldsymbol{Z}_n] = \min[Z_1, Z_2, \ldots, Z_j, \ldots, Z_n] \tag{3}$$

where n is the current excavation stage; and Z_n represents the evaluation error for stage n.

2.3. Back analysis

Back analysis is to combine field measurement and surrogate model prediction to back calculate the parameters affecting the deformation of retaining pile. The first step is to select the key parameters to generate the population. The second step aims to minimize the error function to fulfil the termination criterion or reaching the maximum number of iterations. In the subsequent population calculation, to ensure the consistency with the surrogate model training, the LHS method is applied for sampling within the parameters range as given in Table 4.

The main steps of Level 3 are given as follows.

(1) The Latin hypercube sampling method is used to obtain the initial population of uncertain model parameters.
(2) The generated parameter sets are transferred into Level 2 to establish the BPNN machine learning model. Meanwhile, multi-objective functions are obtained using the trained BPNN model and real measurements.
(3) The multi-objective function values are sorted (with the sorting method explained in Section 2.3) to determine the optimal parameter set within the generated population.
(4) This process is iterated until the stop criterion is fulfilled.

The multi-objective particle swarm optimization (MOPSO) algorithm (Coello and Lechuga, 2002) is applied in the present study. This algorithm has strong global exploration nature, and it is widely used in geotechnical engineering (Dominguez et al., 2014; Tian et al., 2021). This method has two characteristics: (1) adaptive grid searching: it is assumed that i represents the number of grids, and g_i represents the number of particles in the grid. The probability that the particles fall in the grid can be defined as $p_i = 1/g_i$. The more crowded the grid is, the lower the probability is. Hence, the particles track towards the less crowded grids; (2) external repository: the non-dominated sorting is performed on the updated results each time, and the non-inferior solution is saved to the external storage.

When conducting MOPSO, m samples of influence parameters are firstly generated using LHS, which are brought into the BPNN surrogate model (see Section 2.1) to obtain the horizontal displacements of retaining pile. Then, field measurements are utilized for error evaluation. The non-dominated sorting method (Deb et al., 2002) is used to sort the error values with respect to the m samples. The results with lower error values are maintained in the external database, and the rest is eliminated. Finally, when the number of external storages exceeds the threshold, the adaptive grid method is used to sort and eliminate the inferior solutions and to ensure the diversity of the data. The optimal solution is obtained when the termination criterion is fulfilled or the maximum number of iterations is reached.

2.4. Online prediction

For traditional deep excavation problems, the monitoring data are normally investigated when the construction process is already finished. This is because creating a numerical model and conducting parametric study are time-consuming. Hence, field measurements can only be used to assess the efficacy of numerical model, and it cannot act as a guideline during the excavation. Due to this reason, this part of the study proposes an online prediction method, the key feature of which is to adopt the measurements up to the current excavation stage for numerical model evaluation and parameter optimization. Thereafter, the calibrated model parameters are immediately used for prediction of model responses in the next excavation stage. In this way, the currently available measurements can benefit the future excavation stages. It is worth mentioning that the key point for successful operation of online prediction is efficient evaluation of model responses using surrogate model, as well as efficient parameter optimization using MOPSO.

As there are many groups of optimized parameters obtained by back analysis, it is necessary to select a best set of parameters for the subsequent prediction. In this paper, the parameter set with the least cumulative error of all the error functions with respect to each excavation stage is taken as the optimal set. The formula is given as follows:

$$\mathrm{Min}_{\mathbf{pre}} = \min\left[\mathrm{sum}(\boldsymbol{Z}_1, \boldsymbol{Z}_2, \ldots, \boldsymbol{Z}_n)\right] \tag{4}$$

where $\mathrm{Min}_{\mathrm{pre}}$ represents the optimized parameter set with the minimum cumulative error.

3. Case study - Taihu deep excavation

3.1. Project overview

Taihu Lake tunnel is located in Binhu District, Wuxi, China. It is an important channel connecting Mashan Street and Taihu New Town, as shown in Fig. 2. The total length of the tunnel is 10.79 km. The construction began in June 2017, and it is officially open since December 30, 2021. The full section of the tunnel adopts the construction method of dewatering deep foundation pit excavation supported by secant bored piles.

In this study, the selected section (K33 + 960) is in the middle part of the whole Taihu tunnel. According to the geological survey report, there are five layers of strata in the excavation area as seen in Fig. 3. The soil layers are plain fill (layer 1), muddy clay (layer 2), silty clay (layer 3), silty clay (layer 4) and clay (layer 5), and the

corresponding soil parameters are shown in Table 1. The groundwater level is at the surface of plain fill layer, which is stable during the excavation process. The length of the main foundation pit is 43.6 m, and the depth of the foundation pit is 16 m. Retaining pile adopts the technique of bored cast-in-place pile, and its diameter, spacing and length are 1000 mm, 1200 mm and 27 m, respectively.

The excavation is supported by one concrete strut and three steel struts along the depth of the foundation pit (see Fig. 3). The upper one is concrete strut using C30 concrete, and its arrangement is 800 × 1000@5500 mm (the rectangular cross section has a width of 800 mm, height of 1000 mm, and spacing of 5500 mm). The steel struts have the arrangement of Φ609@1200 mm (the circular cross section has a diameter of 609 mm, and spacing of 1200 mm) and a thickness of 12 mm. The structural parameters are shown in Table 2.

During the deep excavation, guide wheel fixed series inclinometer is used to measure the horizontal displacement of retaining pile. The length of inclinometer is 18.5 m, and the interval of series inclinometer is 0.5 m, leading to a total of 37 monitoring points. It is worth mentioning that the horizontal displacement at the bottom of inclinometer is set as 0 to calculate the relative displacement along the retaining pile. From the bottom to the top, the calculation procedure of horizontal displacement shown in Fig. 4 is as follows:

$$L_1 = H_{12} \sin \theta_1 \tag{5}$$

Table 1
Parameters for Hardening Soil constitutive model.

Parameter	Layer 1	Layer 2	Layer 3	Layer 4	Layer 5	Dike
Secant stiffness in triaxial test, E_{50}^{ref} (kN/m^2)	6900	3000	14,000	27,400	13,100	7000
Cohesion, c'_{ref} (kN/m^2)	48.1	7.2	33.8	61.1	73.4	15
Effective friction angle, φ' (°)	14.7	11.4	12.6	17.9	9.5	10
Saturated unit weight, γ_{sat} (kN/m^3)	19.7	17.1	20	20.2	20.2	20

$$L_2 = H_{23} \sin \theta_2 + L_1 \tag{6}$$

$$L_n = H_{nn+1} \sin \theta_n + \sum_1^{n-1} L_i \tag{7}$$

where L_n represents the horizontal displacement of the n th monitoring point; H_{nn+1} represents the distance between the n th and $(n+1)$ th monitoring points (generally a fixed value of 0.5 m). θ_n represents the inclination angle of the connection line between n th and $(n-1)$ th monitoring points.

3.2. Numerical simulation of deep excavation

Based on the field geological survey report and design documents, a PLAXIS 2D (version 2021) FEM is established as seen in Fig. 5. The length of the model is 130 m, and the depth is 36.34 m. It

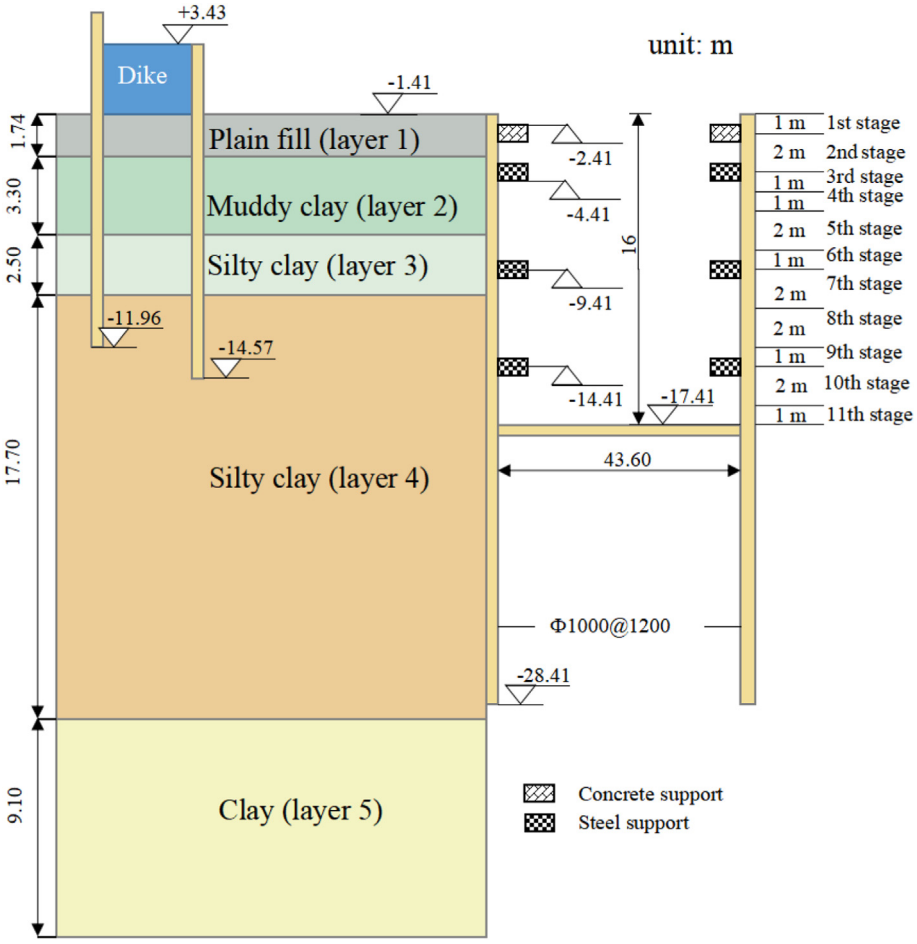

Fig. 3. Stratum distribution and excavation depth of the foundation pit.

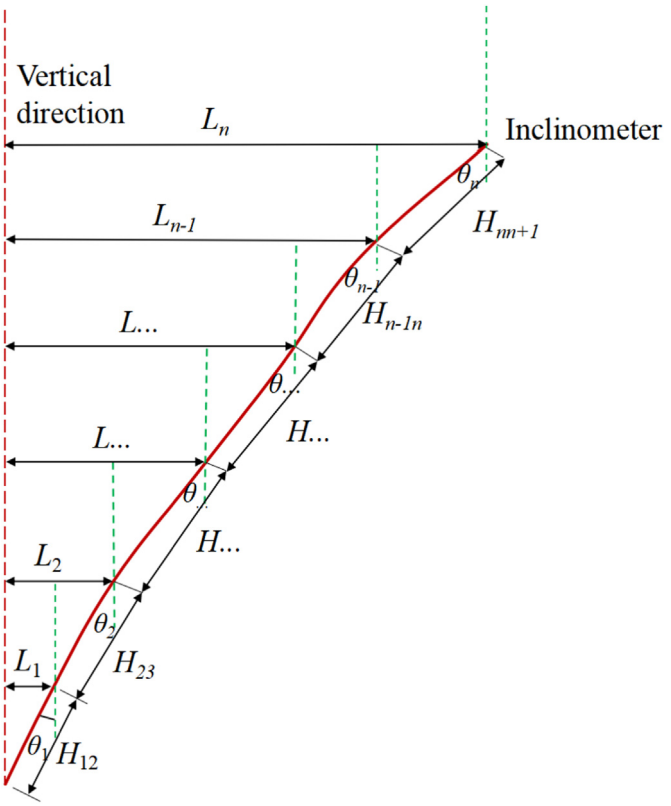

Fig. 4. Principle of pile displacement monitoring.

should be noted that the foundation pit is not symmetric, i.e. the left side of the foundation pit is 10 m away from the dike, and the right side of the foundation pit is 12 m away from the dike. The Hardening Soil model with small-strain stiffness (HSS) is applied in the present study to describe the soil behavior, which has unique advantages in dealing with foundation pit excavation. Li et al. (2019) compared the deformation results of retaining pile in deep excavation using Mohr-Coulomb model and HSS model, and they found that HSS model is more suitable for foundation pit with a depth of more than 15 m. Considering the excavation process in practice, the multi-stage excavation depths are set as 1 m, 3 m, 4 m, 5 m, 7 m, 8 m, 10 m, 12 m, 13 m, 15 m and 16 m.

In the present numerical model, dike cast-in-place pile, cut-off wall, retaining pile and base slab are simulated using plate elements, and concrete support and steel support are simulated using anchor elements. It is worth noting that the project adopts the form of dewatering excavation, dikes are set on both sides of the foundation pit. As seen in Fig. 5, the water levels inside and outside the dike are 0 m and 2 m.

The detailed boundary conditions and assumptions adopted in the numerical model are given as follows:

(1) Boundary conditions. The mechanical boundary conditions at the bottom and outer boundaries of the model are defined by restricting the deformations in the normal direction, while the in-plane displacements are allowed. There is no mechanical fixity on the top surface of the model. Moreover, the model adopts undrained boundary conditions except at the top surface.
(2) Main assumptions. The plane strain condition is adopted in the numerical simulation as the length of the deep excavation is super larger than its width. The soil behavior is described using the HSS, in which the soil is assumed as an isotropic material. The concrete, steel support and retaining pile are assumed as linear elastic materials.

The specific excavation stages in the numerical simulation are defined as follows:

(1) Generate the initial stress field before foundation pit excavation.
(2) Activate the dikes on two sides of the deep excavation.
(3) Activate the cut-off wall and supporting piles.
(4) Step-wise excavation stage (1 m, 3 m, 4 m, 5 m, 7 m, 8 m, 10 m, 12 m, 13 m, 15 m and 16 m). The concrete strut is simultaneously activated after 1 m excavation, and the three steel struts are activated at 4 m, 8 m and 13 m excavation stages. The base slab unit is set up when the excavation is finished.

3.3. Model evaluation

To evaluate the established finite element model, the numerical results of the left retaining pile are compared with the measured horizontal displacements.

3.3.1. Parameter setting

Firstly, the initial FEM parameter set is determined according to the geotechnical report as shown in Table 1. It is worth mentioning that the other parameters, such as E_{oed}^{ref}, E_{ur}^{ref}, and G_0^{ref}, are related to the given parameters. All geological formations in this study are cohesive soil layers. The correlation between each parameter is determined based on relevant literature (Wang et al., 2013; Huang et al., 2015; Zhao et al., 2019):

$$E_{oed}^{ref} = E_{50}^{ref}; E_{ur}^{ref} = 5E_{50}^{ref}; G_0^{ref} = 4E_{ur}^{ref} \quad (8)$$

In addition, Poisson's ratio ($\nu_{ur} = 0.2$) and small strain parameter ($\gamma_{0.7} = 0.0003$) are defined according to the engineering judgement. The structural parameters of pile, strut, and cut-off wall are presented in Table 3.

3.3.2. Numerical results

Fig. 6 shows the numerically calculated horizontal displacements of retaining pile in each stage. It is worth mentioning that

Table 2
Structural parameters for deep excavation.

Structure	Foundation pit bored pile	Concrete strut	Steel strut	Dike bored pile
Material	Concrete	Reinforced concrete	Steel	Concrete
Length (m)	27	43.6	43.6	18
Arrangement	Φ1000@1200 mm	800 × 1000@5500 mm	Φ609@1200 mm	Φ1000@1200 mm

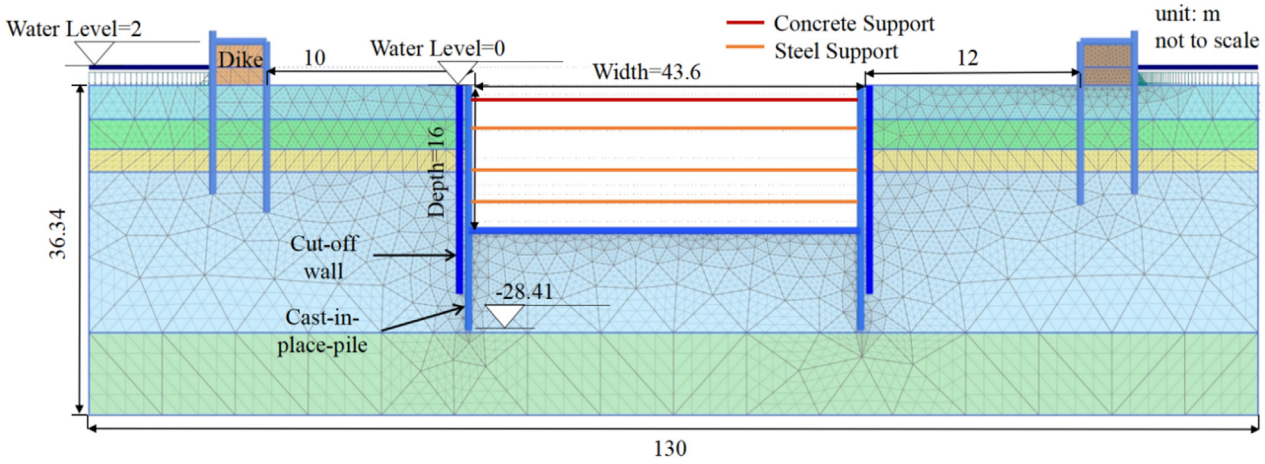

Fig. 5. Geometry and mesh discretization of the finite element model.

Table 3
Construction parameters of the deep excavation.

Parameter	Cut-off wall	Pile	Concrete support	Steel support
EA (kN/m)	2.81×10^7	2.5×10^7	2.47×10^7	6.3×10^6
EI (kN/m)	1.4×10^6	2.1×10^6	–	–
w (kN/m)	3.5	5	–	–
ν_{ur}	0.2	0.2	–	–
$l_{spacing}$ (m)	–	–	8	5.5

Note: EA represents the axial stiffness, EI represents the bending stiffness, w represents the weight of out-of-plane unit width plate, and $l_{spacing}$ represents the spacing between out-of-plane piles.

the numerical results at the bottom of the pile are also set as 0 to calculate the relative displacements along the pile, for comparison with the measured data.

As seen in Fig. 6, the horizontal displacements at different excavation stages basically conform to the deformation law. At the beginning of the excavation, the upper part of the pile deforms rapidly, whilst the lower part of the pile has negligible deformation. This is consistent with the fact that non-excavated areas are supported by the adjacent soil domain. The horizontal displacement of the retaining pile reaches the maximum value at the 10th excavation stage (13 m depth), thereafter the increasing rate of pile displacement at the lower part of the pile gradually becomes higher than that at the upper part of the pile. This results in a decrease of relative pile displacement at the upper part of the pile.

3.3.3. Comparison with the monitoring data

The monitoring data of pile displacements are shown in Fig. 7. The monitoring data at different excavation stages (3 m, 5 m and 7 m) heavily fluctuate, which is attributed to the on-site monitoring noise. Due to this reason, the horizontal displacements of supporting pile in the last five stages are selected in the following investigation. The actual monitoring data are compared with the finite element simulation results, as shown in Fig. 8.

According to Fig. 8, the numerically obtained deformation pattern of retaining pile at each stage is basically in line with the field measurements, demonstrating the applicability of the established finite element model. However, there is large discrepancy between the numerical prediction and the monitoring data. This

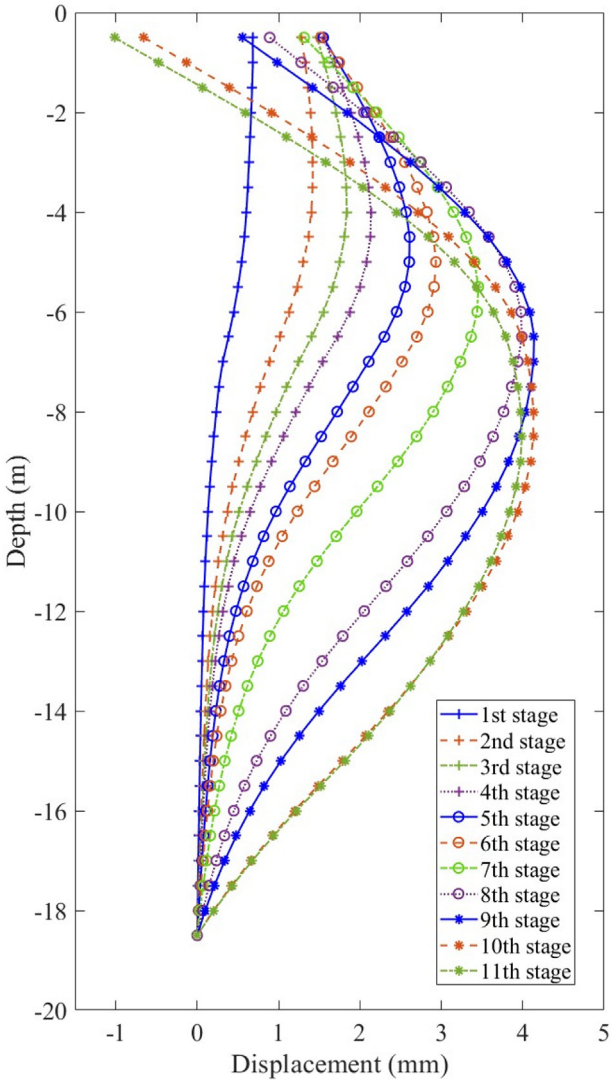

Fig. 6. Numerical simulation results using the initial parameter set.

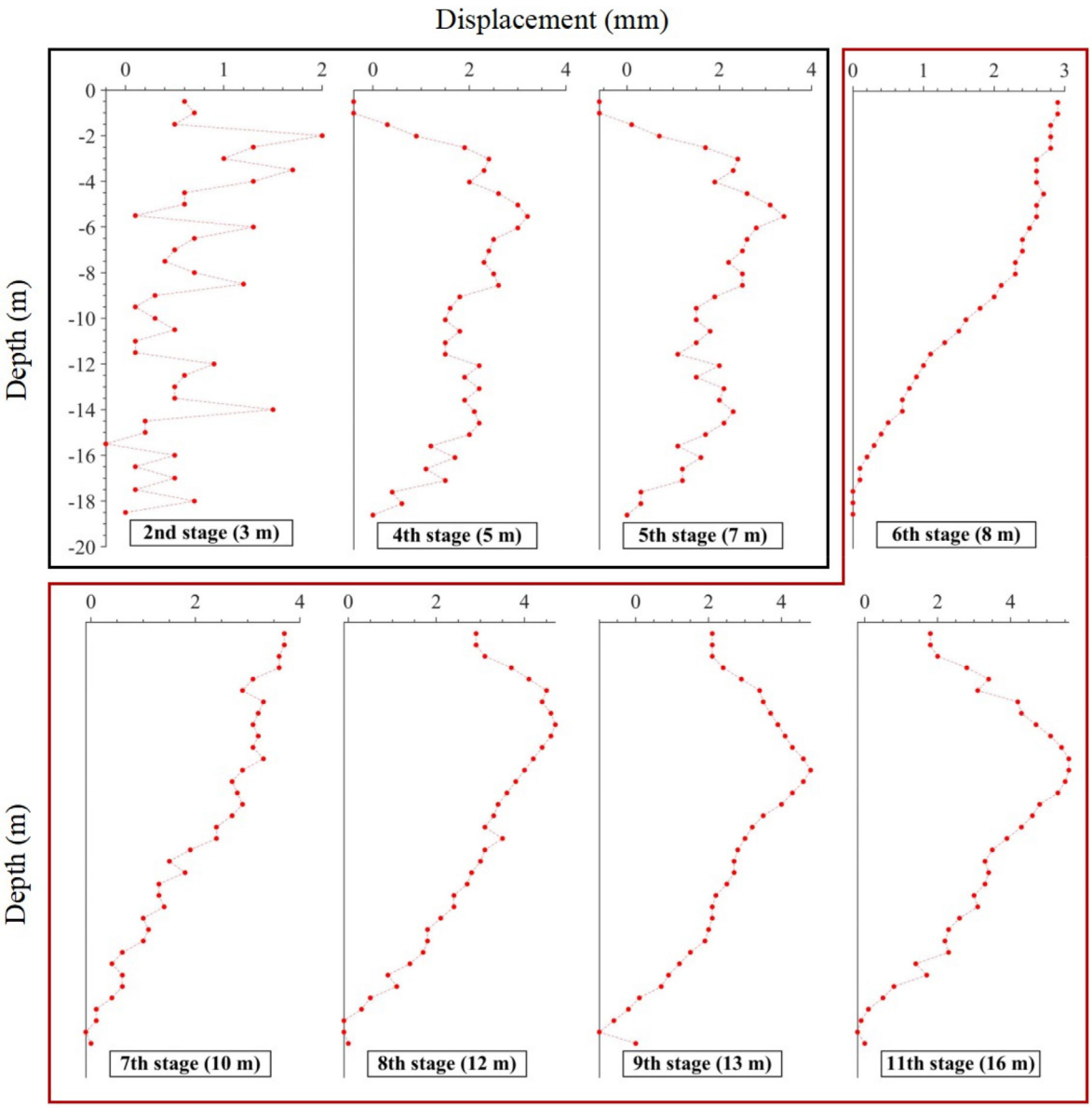

Fig. 7. Monitoring data of pile displacement (black frame for unstable measurements, red frame for stable measurements).

can be attributed to the uncertain soil parameters adopted in the initial numerical analysis.

3.3.4. Parametric study

As mention in Section 2.1, the pile deformation is sensitive to the soil stiffness, cohesion and friction angle. These three parameters are considered in this subsection to conduct parametric study, and the 9th excavation stage (13 m) is taken as an example.

Fig. 9 shows the effect of soil cohesion, friction angle and stiffness parameters, in which the values of $c'_{\mathrm{ref}}, \varphi', E_{50}^{\mathrm{ref}}$ are identical as those in Table 1. As seen in Fig. 9a, the maximum horizontal displacement of retaining pile shows a decreasing trend with increasing the cohesion, and the maximum horizontal displacement is reduced about 12% (from 4.4 mm to 3.85 mm). According to Fig. 9b, when the friction angle increases, the maximum horizontal displacement of retaining pile also shows a decreasing trend, and the maximum value changes from 4.29 mm to 4 mm (about 8% reduction). When the elastic modulus increases (see Fig. 9c), the horizontal displacement at the top of retaining pile shows an increasing trend, and the maximum horizontal displacement of retaining pile shows a decreasing trend. Here, the maximum horizontal displacement of retaining pile decreases from 4.47 mm to 3.84 mm (by about 14%).

According to the above description, the horizontal deformation of retaining pile is more sensitive to the stiffness parameter of the ground domain, which is consistent with the general finding that elastic deformation of the ground domain is more sensitive to the stiffness parameters and also related to the shear parameters (Zhao et al., 2015). To resolve the discrepancy between numerical prediction and field monitoring data, back analysis-based optimization is conducted in the following sections.

3.4. Back analysis and online prediction

3.4.1. Latin hypercube sampling

As mentioned before, sensitive parameters in determining the horizontal displacements of retaining pile are divided into three groups, including stratum parameters (i.e. elastic modulus E,

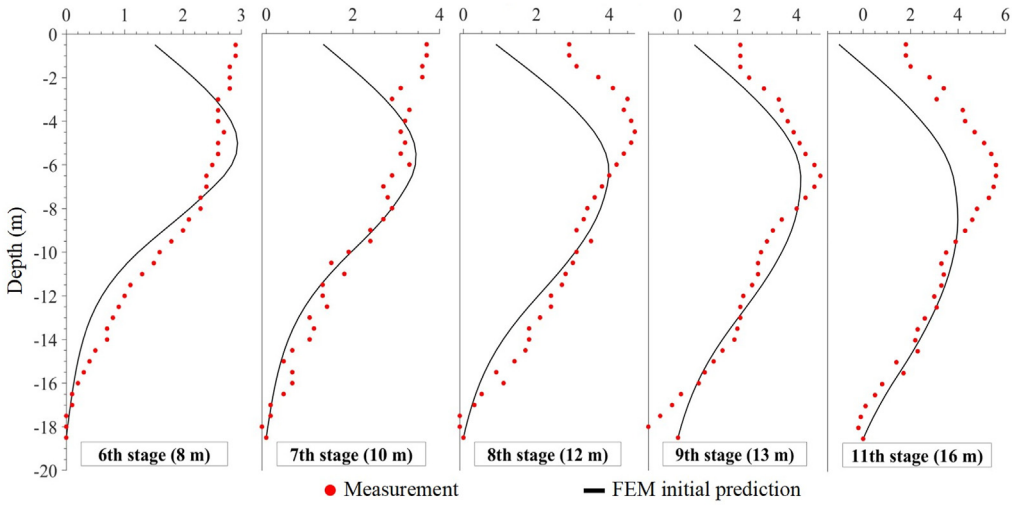

Fig. 8. Comparison between field measurements and numerical simulations.

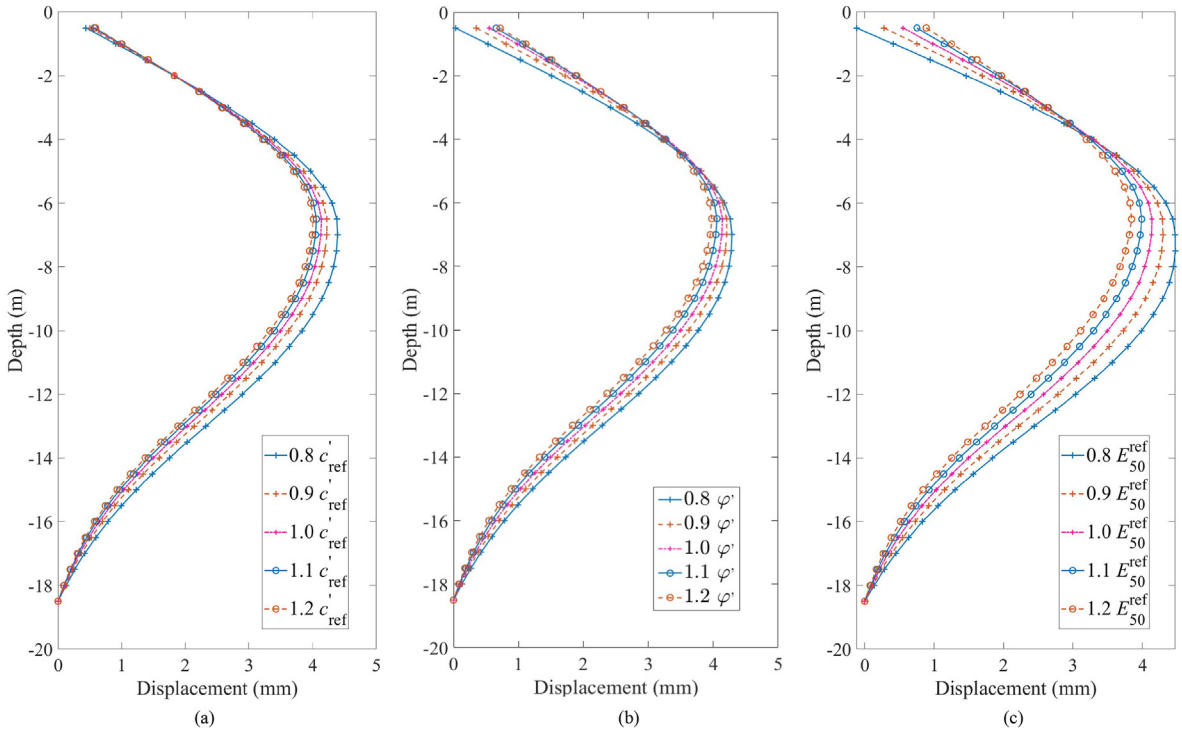

Fig. 9. Effect on the horizontal displacement of retaining pile at the 9th excavation stage: (a) Cohesion, (b) Friction angle, and (c) Stiffness.

cohesion c, and internal friction angle φ), structural parameters (i.e. supporting strut stiffness) and construction parameters (i.e. excavation depth in each stage). According to the geotechnical report, the ranges of all considered possible parameter combinations are shown in Table 4. A total of 200 parameter groups are sampled, and each group consists of 18 parameters (including the excavation depth).

3.4.2. Establishment of BPNN

This study uses Python code to build a BPNN model as shown in Fig. 10. The number of neurons is 144, and it has two hidden layers and each has 72 neurons. The activation functions of the hidden layer and output layer are "ReLU" (Rectified Linear Unit) and "Linear", respectively. The optimization function adopts the adaptive stochastic gradient algorithm, Adam (Kingma and Ba, 2015), which is an extension of the stochastic gradient descent method. Recently, the Adam algorithm has been widely used in deep learning applications in computer vision and natural language processing. In addition, 70% of the data are used for training and the rest is applied in test.

To eliminate the influence of the order of magnitude, the input parameters (a total of 18 features) are normalized. Then, the BPNN model consisting of influencing factors and horizontal displacements of retaining pile are established. After successful training, the performance of BPNN model at a depth of 0.5 m along the pile is shown in Fig. 11 as an example. Fig. 12 further shows the coefficient

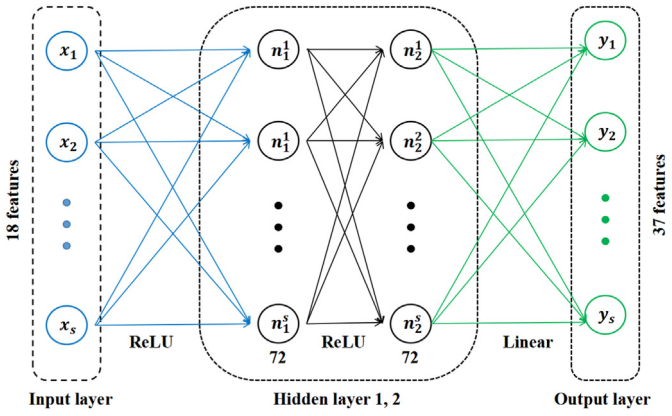

Fig. 10. Construction of a neural network.

Table 4
Ranges of uncertain soil and structural parameters.

Adopted range	Layer 1	Layer 2	Layer 3	Layer 4	Layer 5
E_{50}^{ref} (kN/m^2)	3000 −20,000	1000 −10,000	3000 −25,000	3000 −40,000	3000 −30,000
c'_{ref} (kN/m^2)	10–50	3–30	10–80	10–100	20–100
φ' (°)	3–30	0.5–15	1–30	3–35	3–35
$E_{concrete}$ (kN/m^2)	3×10^7–5×10^7				
E_{steel} (kN/m^2)	2×10^8–3×10^8				

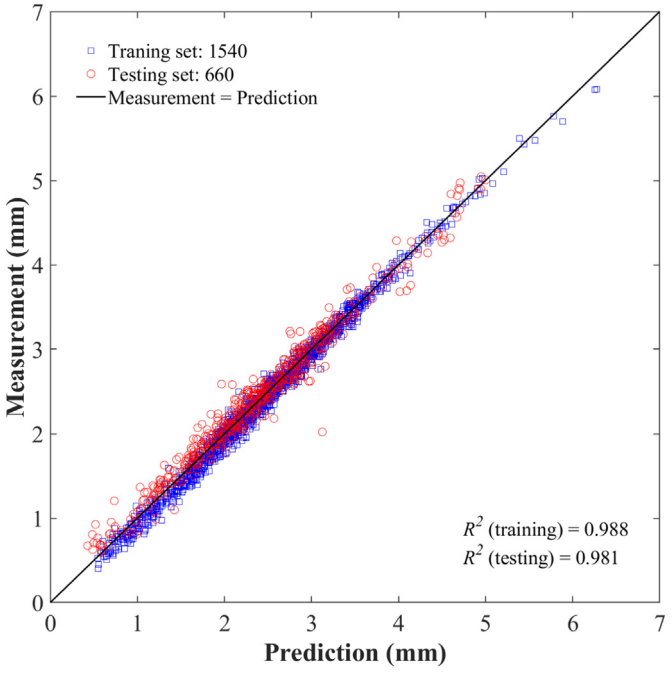

Fig. 11. Comparison between measured and BPNN model predicted pile horizontal displacements at a depth of 0.5 m.

of determination (R^2) for all other 37 monitoring points along the pile. As seen, the BPNN model accuracy is more than 90%. Moreover, Fig. 13 plots the MSE against epoch. Here, MSE is defined as $\sum_1^n (f(x) - y)/n$, which is used as an optimization indicator for training, and epoch is one complete cycle for BPNN being trained and tested once. Here, $f(x)$ is the result of the neural network, and y is the FEM result. It can be seen that the accuracy of BPNN surrogate model is gradually stable after 80 epochs.

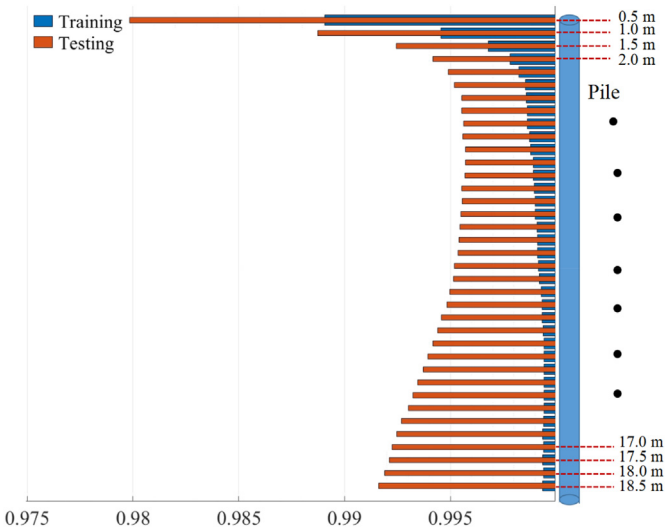

Fig. 12. Errors for both training and testing sets at 37 monitoring points along the pile depth.

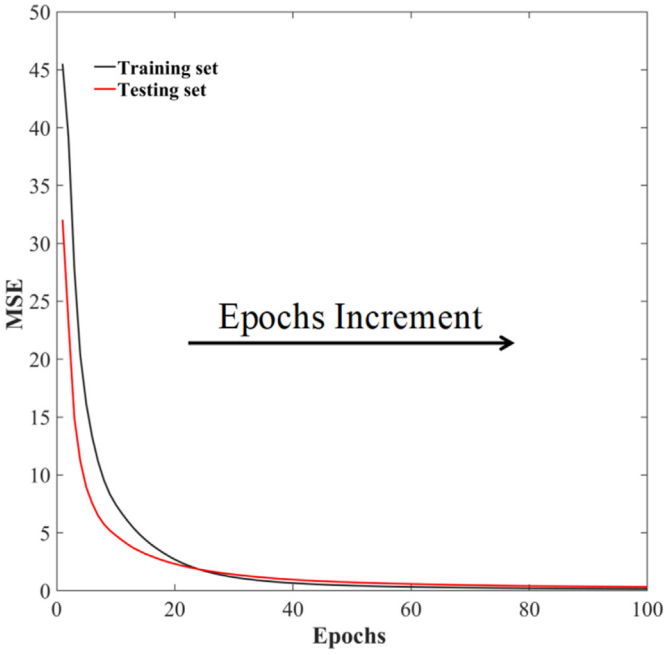

Fig. 13. MSE versus epoch during training of the BPNN model.

3.4.3. Back analysis

The back analysis approach has been explained in detail in Section 2. In this Taihu excavation project, five groups of monitoring data (excavation depths: 8 m, 10 m, 12 m, 13 m and 16 m) are selected. To make full use of these measurements, the multi-objective functions are defined as seen in Table 5.

3.4.4. Online prediction

Online prediction is to use the monitoring data from previous excavation stages to optimize the model parameters and to predict the displacement of retaining pile in a subsequent excavation stage. The details have been described in Section 2.

Table 5
Error function definition.

Two-objective optimization	Z_8, Z_{10}
Three-objective optimization	Z_8, Z_{10}, Z_{12}
Four-objective optimization	Z_8, Z_{10}, Z_{12}, Z_{13}

Figs. 14–16 show the results of two-objective, three-objective and four-objective optimization, respectively. The black box represents the monitoring data involved in back analysis, and the red box represents the prediction results. Generally, the predictions using the optimized parameters can well match the field measurements, which means that the online prediction approach has a sufficient high accuracy (more than 90%). Furthermore, with increasing amount of monitoring data, the online prediction accuracy for subsequent excavations can also be improved. For example, the prediction accuracy at 16 m excavation stage increases from 0.8731 for two-objective optimization to 0.9463 for four-objective optimization.

It is worth noting that the performance of the initial FEM at all excavation stages is not acceptable. In contrast, the proposed deep learning based multi-objective online optimization method has a sufficient high accuracy at all excavation stages. In addition, the computational costs for multi-objective optimization are comparable (less than 3 min difference). Therefore, it is recommended to use all monitoring data during the excavation process for parameter optimization to cover all information that could be ignored in the previous excavation stages.

As mentioned before, online prediction requires efficient evaluation of pile displacement under certain parameter combination. BPNN plays an important role in the proposed online prediction approach, as it significantly reduces the computational cost in the entire process as presented in Table 6.

In this present project, there are 17 parameters that need to be identified. Based on the results of trial analysis, about 500 iterations are required in back analysis to obtain a reliable optimization solution. This means that in the traditional method, one needs to run the FEM for 501 times (one run for the initial population calculation), which costs about 5010 min. Nevertheless, when the surrogate model is trained successfully in advance, only the surrogate model is analyzed in each iteration, and the total computational

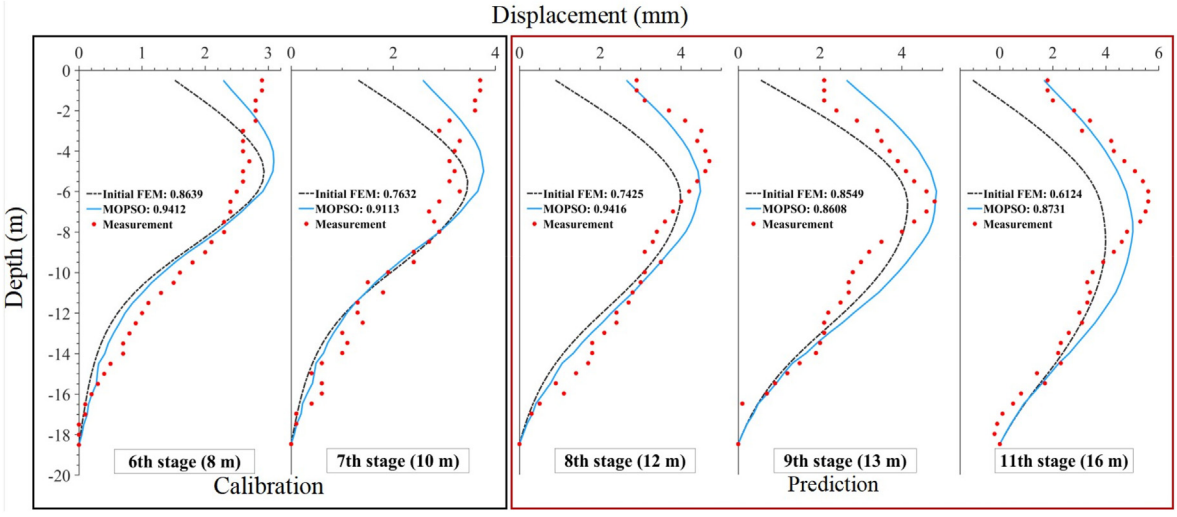

Fig. 14. Two-objective optimization results (black frame for calibration, red frame for prediction).

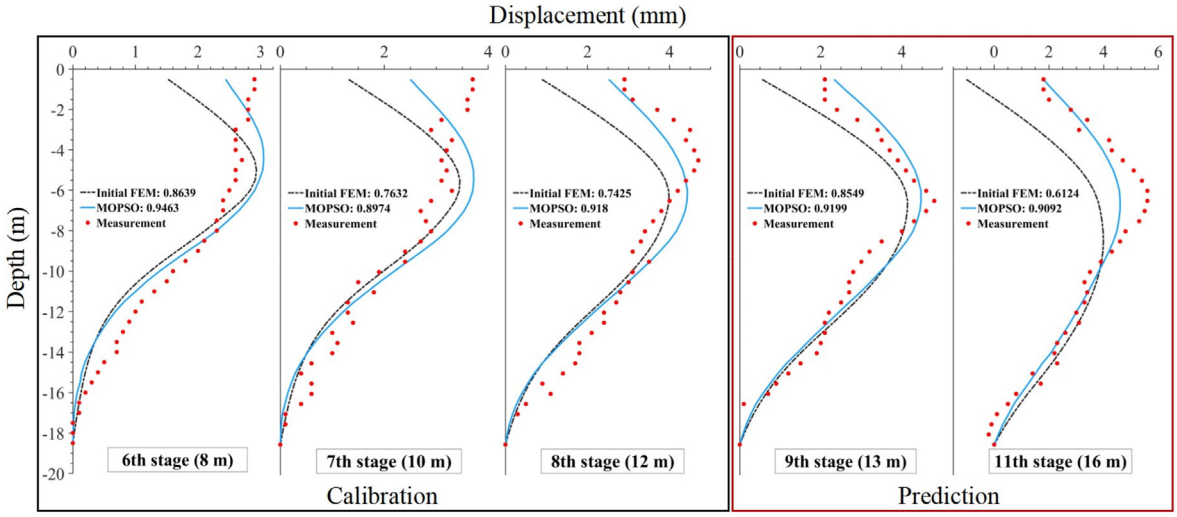

Fig. 15. Three-objective optimization results (black frame for calibration, red frame for prediction).

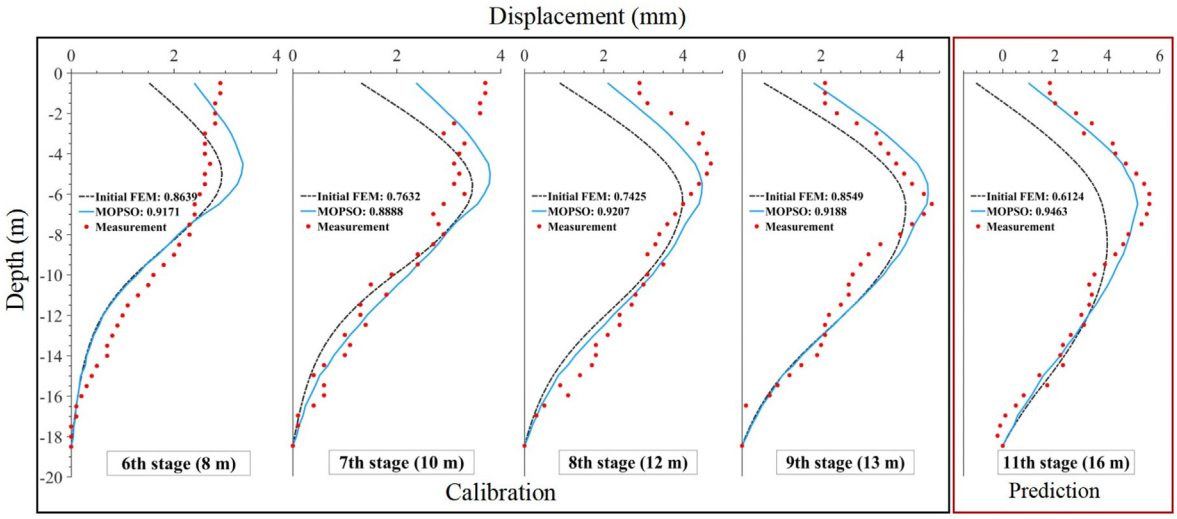

Fig. 16. Four-objective optimization results (black frame for calibration, red frame for prediction).

Table 6
Comparison of computational time for calculations using traditional and BPNN-based multi-objective optimization methods.

Item	Before excavation	During excavation		
	Surrogate model training	Number of runs in optimization	Calculation time for each run	Total time
Traditional multi-objective optimization	–	500	10 min	$(500+1)\times 10 = 5010$ min
Multi-objective optimization using BPNN	$200\times 10 = 2000$ min	500	2 s	$(500+1)\times 2 = 1002$ s

time is only 1002 s. Compared with the traditional method, the computational cost using the proposed method is reduced by more than 95%. If the reliable optimization result is not yet obtained after 500 iterations, the advantage of the surrogate model can be more prominent.

4. Discussions

In addition to the MOPSO algorithm, another two popular algorithms, namely NSGA-II (Deb et al., 2002) and Pareto Envelope-based Selection Algorithm II (PESA-II) (Corne et al., 2001), are applied in this part of the study for comparison. Using the same procedure mentioned in Fig. 1 for online prediction, the analysis results of two-objective, three-objective, and four-objective optimization tasks are shown in Figs. 17–19, respectively. The model accuracy for predicting pile displacements at 16-m excavation stage is further presented in Table 7.

According the prediction results, when more objective functions are considered, the model accuracy using NSGA-II algorithm reduces from 0.8889 to 0.812, which reflects the disadvantage of the NSGA-II algorithm. On the contrary, the MOPSO algorithm accuracy gradually increases from 0.8731 to 0.9463, when the dimension of optimization problem increases. The performance of PESA-II algorithm is intermediate, and its accuracy is slightly affected by the number of dimensions in multi-objective optimization.

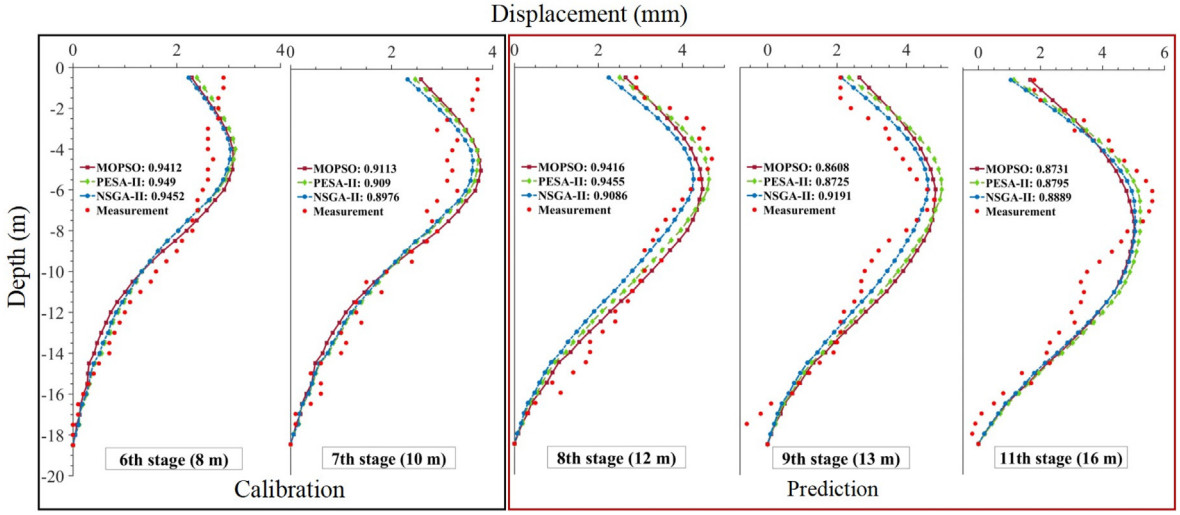

Fig. 17. Two-objective optimization using different algorithms (black frame for calibration, red frame for prediction).

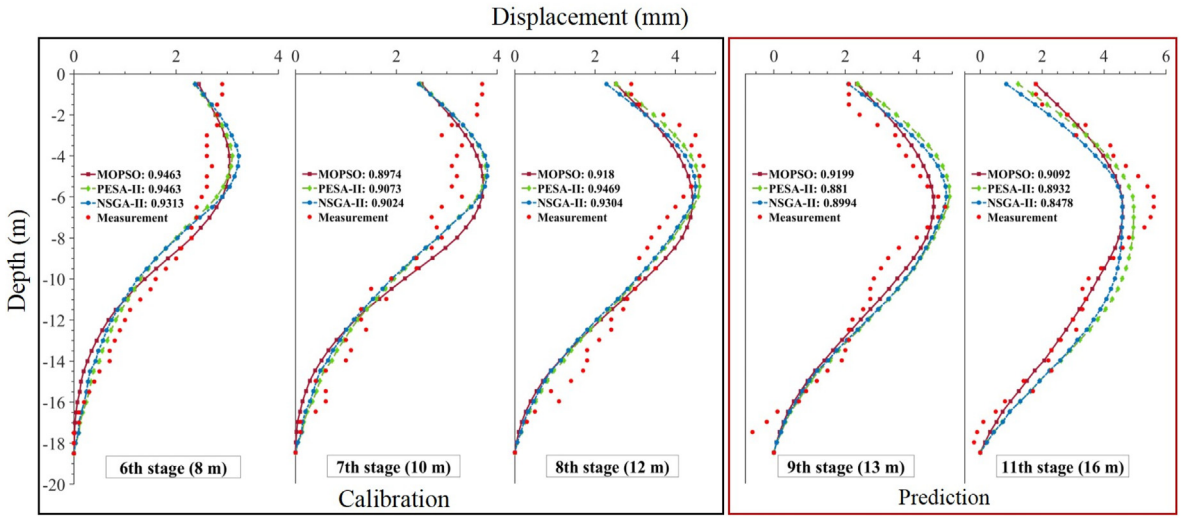

Fig. 18. Three-objective optimization using different algorithms (black frame for calibration, red frame for prediction).

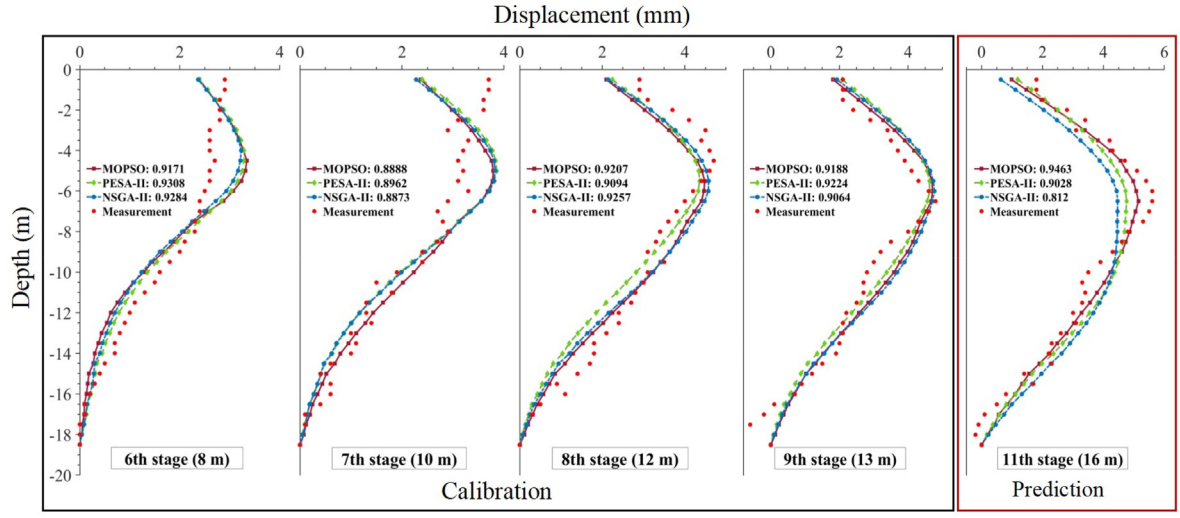

Fig. 19. Four-objective optimization using different algorithms (black frame for calibration, red frame for prediction).

There are two differences between NSGA-II and PESA-II, MOPSO algorithms. Firstly, the latter two algorithms set up an external database to store the non-dominated solution sets. Secondly, the new population for NSGA-II is generated from the entire dataset. On the contrary, the new population for PESA-II and MOPSO is generated from the external database only. As shown in Fig. 20, in a 2D problem, the 0, 1, …, n levels are separated using the non-dominated sorting method (Deb et al., 2002). Here, the 0 level represents the non-dominated set, which is stored in the external database for the PESA-II and MOPSO algorithms.

For the high dimensional objective case (objectives), when certain objective is not dominated, its error function value is small. Assuming that the ratio of dominated and non-dominated objectives is 1:1, in case n objectives are considered, the proportion of non-dominated solution sets among all solution set is $1/2^n$. When the proportion of non-dominated solution set (external database) decreases with increasing number of the objectives (error function), NSGA-II algorithm cannot fully consider the non-dominated solution set for generating a new population, eventually resulting in a reduction of model accuracy. When PESA-II and MOPSO generate a new population, the dominant solution set (Rank = 1, 2, …, n in Fig. 19) is eliminated. This makes the algorithm focus on the non-dominant solution set, which results in an improvement of the accuracy in comparison to NSGA-II.

By analogy, for the low dimensional objectives, for example $n = 2$, the proportion difference between the dominant set and the non-dominant set is negligible. The NSGA-II algorithm considers the entire dataset to obtain the global optimum. Hence, NSGA-II algorithm shows the better performance than the other two algorithms (see Table 7).

According to the above discussions, the following advices are suggested for engineering practice.

(1) When the monitoring data at all previous excavation stages are available, if one needs to predict the system behavior in the next excavation stage, it is suggested to apply the MOPSO algorithm.
(2) If one needs to predict the final displacements with limited monitoring data at the beginning excavation stages, the NSGA-II algorithm is recommended.

Table 7
Accuracy and time cost of different algorithms for multi-objective optimization problems (prediction of pile displacement at an excavation depth of 16 m).

Algorithm	Two-objective	Three-objective	Four-objective	Time (s)
MOPSO	0.8731	0.9092	0.9463	1187
PESA-II	0.8795	0.8932	0.9028	1366
NSGA-II	0.8889	0.8478	0.812	1677

Note: The calculation time refers to the four-objective optimization task.

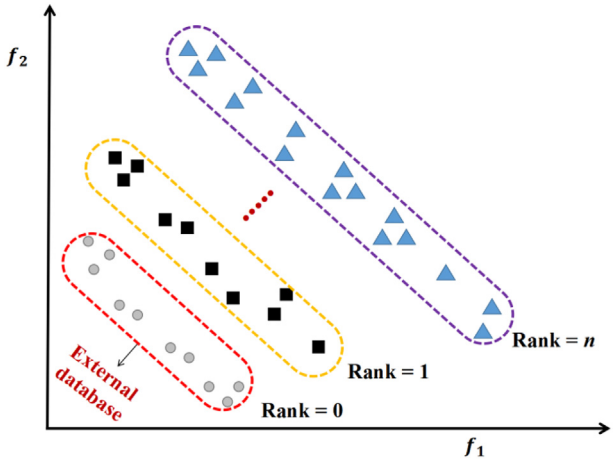

Fig. 20. Conceptual illustration of the proposed optimization algorithm (f_1 and f_2 represent the first and second objective function values, respectively).

(3) When the construction speed is fast, if one needs to quickly achieve online prediction, it is recommended to use the MOPSO algorithm.

It is worth mentioning that this method can be applied not only to deep excavation applications, but also to any other practical problems involving finite element simulations. This technique offers the flexibility of choosing different finite element simulation tools or optimization algorithms for specific engineering problems.

5. Conclusions

A modified multi-objective optimization procedure is proposed in this paper, which combines multi-objective optimization (MOPSO) algorithm and back analysis method to improve the optimization accuracy. The BPNN method is further applied to substitute the FEM calculation during back analysis. In this way, the proposed approach can achieve an efficient online prediction. The proposed procedure is further applied in the Taihu Tunnel excavation project to demonstrate its effectiveness and accuracy. The specific contents are as follows:

(1) A fine FEM is established to simulate the construction process of Taihu tunnel excavation. The numerical results are compared with the measured horizontal displacements of retaining pile to show the consistent deformation trends, demonstrating the reliability of the finite element model.
(2) A surrogate model using BPNN algorithm is developed to substitute the finite element simulation of Taihu tunnel excavation. The trained robust BPNN model has an accuracy above 90%.
(3) Compared with the traditional multi-objective optimization approach, the computational cost is reduced by approximately 95% via implementing BPNN algorithm into multi-objective optimization. The real-time prediction accuracies of pile displacement at all excavation stages are more than 90%. This makes the online prediction of system behavior available and affordable.
(4) The MOPSO algorithm generally performs better than the PESA-II and NSGA-II algorithms. It is suggested to apply the MOPSO method, in case one needs to predict the system behavior in the next excavation stage based on the continuously increasing monitoring data.

Declaration of competing interest

The authors declare that they have no known competing financial interests or personal relationships that could have appeared to influence the work reported in this paper.

Acknowledgments

This work was supported by the National Natural Science Foundation of China (Grant Nos. 52208380 and 51979270), and the Open Research Fund of State Key Laboratory of Geomechanics and Geotechnical Engineering, Institute of Rock and Soil Mechanics, Chinese Academy of Sciences (Grant No. SKLGME021022). The authors gratefully acknowledge these supports.

References

Cao, M.S., Pan, L.X., Gao, Y.F., Novak, D., Ding, Z.C., Lehky, D., Li, X.L., 2017. Neural network ensemble-based parameter sensitivity analysis in civil engineering systems. Neural Comput. Appl. 28, 1583–1590.
Coello, C.A.C., Lechuga, M.S., 2002. MOPSO: a proposal for multiple objective particle swarm optimization. In: Proceedings of the 2002 Congress on Evolutionary Computation. IEEE, New York, pp. 1051–1056.
Corne, D.W., Jerram, N.R., Knowles, J.D., Oates, M.J., 2001. PESA-II: region-based selection in evolutionary multiobjective optimization. In: Proceedings of the 3rd Annual Conference on Genetic and Evolutionary Computation, pp. 283–290.
Deb, K., Pratap, A., Agarwal, S., Meyarivan, T., 2002. A fast and elitist multiobjective genetic algorithm: NSGA-II. IEEE Trans. Evol. Comput. 6, 182–197.
Dominguez, M., Fernandez-Cardador, A., Cucala, A.P., Gonsalves, T., Fernandez, A., 2014. Multi objective particle swarm optimization algorithm for the design of efficient ATO speed profiles in metro lines. Eng. Appl. Artif. Intell. 29, 43–53.
Feng, Z., Xu, Q., Xu, X., Tang, Q., Li, X., Liao, X., 2022. Deformation characteristics of soil layers and diaphragm walls during deep foundation pit excavation: simulation verification and parameter analysis. Symmetry-Basel. 14, 254.
Gao, W., Lu, X., Peng, Y., Wu, L., 2020. A deep learning approach replacing the finite difference method for in situ stress prediction. IEEE Access 8, 44063–44074.
He, X., Wang, F., Li, W., Sheng, D., 2021. Efficient reliability analysis considering uncertainty in random field parameters: trained neural networks as surrogate models. Comput. Geotech. 136, 104212.
Hong, L., Wang, X., Zhang, W., 2023. Reliability-based robust geotechnical design of braced excavations considering multiple failure modes. Undergr. Space 9, 43–52.
Huang, Z.H., Zhang, L.L., Cheng, S.Y., Zhang, J., Xia, X.H., 2015. Back-analysis and parameter identification for deep excavation based on Pareto multiobjective optimization. J. Aero. Eng. 28, A4014007.
Jiang, A.N., Wang, S.Y., Tang, S.L., 2011. Feedback analysis of tunnel construction using a hybrid arithmetic based on Support Vector Machine and Particle Swarm Optimisation. Autom. ConStruct. 20, 482–489.
Jiang, S.H., Papaioannou, I., Straub, D., 2018a. Bayesian updating of slope reliability in spatially variable soils with in-situ measurements. Eng. Geol. 239, 310–320.
Jiang, Q., Sun, Y., Yi, B., Li, T., Xiong, F., 2018b. Inverse analysis for geomaterial parameter identification using Pareto multiobjective optimization. Int. J. Numer. Anal. Methods GeoMech. 42, 1698–1718.
Jiang, X., Zong, J., Sun, L., 2007. Construction monitoring and numerical simulation for a deep excavation in Tianjin. J. China Civil Eng. 40 (2), 79–84.
Jin, Y.F., Yin, Z.Y., Zhou, W.H., Huang, H.W., 2019. Multi-objective optimization-based updating of predictions during excavation. Eng. Appl. Artif. Intell. 78, 102–123.
Jin, Y.-F., Yin, Z.Y., Zhou, W.H., Liu, X., 2020. Intelligent model selection with updating parameters during staged excavation using optimization method. Acta Geotech 15, 2473–2491.
Kingma, D.P., Ba, J., 2015. Adam: a method for stochastic optimization. 3rd International Conference on Learning Representations, ICLR 2015, San Diego, CA, USA.

Kung, G.T.C., Ou, C.Y., Juang, C.H., 2009. Modeling small-strain behavior of Taipei clays for finite element analysis of braced excavations. Comput. Geotech. 36, 304–319.
Li, L.X., Liu, J.D., Li, K.J., Huang, H.L., Ji, X.K., 2019. Study of parameters selection and applicability of HSS model in typical stratum of Jinan. Rock Soil Mech. 40, 4021–4029.
Liu, X., Hussein, S.H., Ghazali, K.H., Tung, T.M., Yaseen, Z.M., Xin, B., 2021. Optimized adaptive neuro-fuzzy inference system using metaheuristic algorithms: application of shield tunnelling ground surface settlement prediction. Complexity 2021, 6666699.
Mohamad, E.T., Armaghani, D.J., Momeni, E., Yazdavar, A.H., Ebrahimi, M., 2018. Rock strength estimation: a PSO-based BP approach. Neural Comput. Appl. 30, 1635–1646.
Park, H.I., Kim, K.-S., Kim, H.Y., 2015. Field performance of a genetic algorithm in the settlement prediction of a thick soft clay deposit in the southern part of the Korean peninsula. Eng. Geol. 196, 150–157.
Qian, T., Gong, X., Li, Y., 2011. Analysis of braced excavation with pit-in-pit based on orthogonal experiment. In: Sun, D., Sung, W.P., Chen, R. (Eds.), Frontiers of Green Building, Materials and Civil Engineering, Pts 1-8. Trans Tech Publications Ltd, Stafa-Zurich, pp. 4549–4553.
Qian, W., Chai, J., Qin, Y., Xu, Z., 2019. Simulation-optimization model for estimating hydraulic conductivity: a numerical case study of the Lu Dila hydropower station in China. Hydrogeol. J. 27, 2595–2616.
Rumelhart, D.E., Hintont, G.E., Williams, R.J., 1986. Learning representations by back-propagating errors 4. Nature 323, 533–536.
Song, E.X., Lou, P., Lu, X.Z., 2004. Nonlinear 3D finite element analysis of an extremely deep excavation support system. Rock Soil Mech. 25 (4), 538–543.
Stone, R.C., Farhangi, V., Fatahi, B., Karakouzian, M., 2023. A novel short pile foundation system bonded to highly cemented layers for settlement control. Can. Geotech. J. https://doi.org/10.1139/cgj-2020-0710.
Sun, Y., Jiang, Q., Yin, T., Zhou, C., 2018. A back-analysis method using an intelligent multi-objective optimization for predicting slope deformation induced by excavation. Eng. Geol. 239, 214–228.
Tao, R., Daan, L., Songhua, M., Weiwei, W., Lihua, T., 2019. Intelligent feedback analysis on a deep excavation for the gravity anchorage foundation of a super suspension bridge. Chin. J. Rock Mech. Eng. 38, 2898–2912.
Tao, Y., He, W., Sun, H., Cai, Y., Chen, J., 2022. Multi-objective optimization-based prediction of excavation-induced tunnel displacement. Undergr. Space 7, 735–747.
Tian, Z., Zhang, Z., Zhang, K., Tang, X., Huang, S., 2021. Statistical modeling and multi-objective optimization of road geopolymer grouting material via RSM and MOPSO. Construct. Build. Mater. 271, 121534.
Wang, R., Liu, S., Xu, L., Zhao, C., Ni, P., Zheng, W., 2022. Performance of a 56m deep circular excavation supported by diaphragm and cut-off double-wall system in shanghai soft ground. Can. Geotech. J. 60 (4). https://doi.org/10.1139/cgj-2022-0308.
Wang, W., Wang, H., Xu, Z., 2013. Research on soil HS-Small model parameters in numerical analysis of foundation pit excavation in Shanghai. Geotech. Mech. 34, 1766–1774.
Wu, B., Zhang, Z.Y., Huang, W., 2021. Sensitivity analysis of stability parameters of foundation pit in sandy soil stratum based on orthogonal test. J. Saf. Sci. Technol. 17, 128–134.
Xue, X., 2017. Prediction of slope stability based on hybrid PSO and LSSVM. J. Comput. Civ. Eng. 31, 04016041.
Zhang, L., Shi, B., Zhu, H., Yu, X.B., Han, H., Fan, X., 2021. PSO-SVM-based deep displacement prediction of Majiagou landslide considering the deformation hysteresis effect. Landslides 18, 179–193.
Zhang, W., Goh, A.T.C., Zhang, Y., 2015. Updating soil parameters using spreadsheet method for predicting wall deflections in braced excavations. Geotech. Geol. Eng. 33, 1489–1498.
Zhao, B.D., Zhang, L.L., Jeng, D.S., Wang, J.H., Chen, J.J., 2015. Inverse analysis of deep excavation using differential evolution algorithm. Int. J. Numer. Anal. Methods GeoMech. 39, 115–134.
Zhao, C., Alimardani Lavasan, A., Barciaga, T., Schanz, T., 2019. Mechanized tunneling induced ground movement and its dependency on the tunnel volume loss and soil properties. Int. J. Numer. Anal. Methods GeoMech. 43, 781–800.
Zhao, C., Mahmoudi, E., Luo, M., Jiang, M., Lin, P., 2023. Unfavorable geology recognition in front of shallow tunnel face using machine learning. Comput. Geotech. 157, 105313.
Zhu, H.H., Yang, L., Tadashi, H., 1998. Back analysis of construction of deep excavation and horizontal displacement prediction. Chin. J. Rock Mech. Eng. 20 (4), 30–35.
Zhu, H.H., Liu, X., 2003. Comparison study of mixed optimal methods based on genetic algorithm in back analysis. Chin. J. Rock Mech. Eng. 22 (2), 197–202.

Dr. Chenyang Zhao obtained his Ph.D. at Ruhr University Bochum (Germany) on refined numerical simulation of mechanized tunneling. He is now Assistant Professor at Sun Yat-sen University (China). He developed expertise in numerical simulation, machine learning and soil-structure interaction.